

Tidally Delayed Spin-Down of Very Low Mass Stars

Ketevan Kotorashvili^{1,2*} and Eric G. Blackman^{1,2*}

^{1*}Department of Physics and Astronomy, University of Rochester, 500 Wilson Boulevard, Rochester, 14627, NY, USA.

²Laboratory for Laser Energetics, University of Rochester, 250 East River Road, Rochester, 14623, NY, USA.

*Corresponding author(s). E-mail(s): kkotoras@ur.rochester.edu; blackman@pas.rochester.edu;

Abstract

Very low-mass main-sequence stars reveal some curious trends in observed rotation period distributions that require abating the spin-down that standard rotational evolution models would otherwise imply. By dynamically coupling magnetically mediated spin-down to tidally induced spin-up from close orbiting substellar companions, we show that tides from sub-stellar companions may explain these trends. In particular, brown dwarf companions can delay the spin-down and explain the observed bimodality in rotation period distribution of old, late-type M stars. We find that tidal forces also strongly influence stellar X-ray activity evolution, so that methods of gyrochronological aging must be generalized for stars with even sub-stellar companions. We also discuss how the theoretical predictions of the spin evolution model can be used with future data to constrain the population distribution of companion orbital separations.

The observed period distributions of main sequence stars as a function of age constrain models of stellar spin evolution. In turn, understanding the spin evolution is important for gyrochronological aging [1, 2], which depends on a one-to-one mapping between rotation period and stellar age, bolstered by a predictive theory. However, observations reveal that the rotation and activity of significant populations of main sequence stars evolve anomalously with age [3–5], challenging standard theoretical models restricted to the magnetically mediated spin down of isolated stars [2, 6–10]. The anomalies include: (i) a gap in the rotation period distributions at intermediate rotation periods

among G dwarfs, K-dwarfs, up to early-M dwarfs [11]; (ii) a rapid rise and fall in the rotational periods of late and early K-type stars during their early main sequence (MS) phase [12]; (iii) a bimodal distribution in rotation period for late-type M dwarfs, lacking stars with intermediate periods [13, 14]. [11, 13, 14].

While a change in magnetic topology might help to explain some anomalies [15], many stars have stellar, substellar, or planetary companions whose influence on spin angular momentum evolution must also be understood. M dwarfs with short rotation periods may either be very young, or involve short-period stellar binaries [11]. Using galactic kinematics to estimate M dwarf ages, there is indeed a sub-population of fast-rotating old stars (7 – 13 Gyr) [13]. The presence of a sufficiently massive companion can modify the spin evolution of the host stars via equilibrium and dynamical tides [16–19] and generate the bimodal rotation period distribution. As we explore here, even sub-stellar brown dwarf (BD) companions may be sufficient to explain the observations,

In contrast to semi-empirical [9] or semi-analytical and numerical magnetohydrodynamic models [20–22], our model herein dynamically couples the evolution of X-ray luminosity, rotation, mass loss, magnetic field strength to tidal effects of the companion and its orbital evolution. Previous work has also focused on solar-type stars and the effects of core-envelope decoupling in studying the influence of a massive planet on the stellar surface rotation [20, 21]. Here we study the influence of tides on the stellar spin evolution of fully convective M dwarf-BD systems for a range of companion masses and orbital separations. We focus on explaining the bimodality of rotation period distribution for late-type M dwarfs [11, 13, 14] by accounting for equilibrium tides. For comparison, we also investigate the spin evolution implications of sub-BD mass companions for partially convective K dwarfs and early M dwarfs.

1 Results

1.1 Description of systems studied

To study M dwarf-BD and K dwarf-Jupiter mass companion systems we extend the minimalist theoretical spin evolution model [23], which dynamically couples stellar spin, magnetic field strength, X-ray luminosity and mass loss to include tidal interactions. We numerically solve the generalized system of equations (1), (2), (4) or (5), (7), (15) and (17) derived in section 3, which describes the stellar spin evolution when spin-down due to magnetic braking is coupled to tides. For all investigations below, we compare cases with both magnetic braking and tides to cases with just magnetic braking. For the latter, we solve equation (3) instead of equations (15) and (17). Our model parameters are given in section 3.4 and the initial system properties for each case are given in Table 1. Using these values, we vary the companion mass and fix the initial value of the orbital separation, or vice versa. We define the initial orbital separation a_i as a fraction p_f of the corotation radius $a_i = p_f R_{co}$, where the corotation radius is given by $R_{co} = (GM_\star/\Omega_\star^2)^{1/3}$, G is the gravitational constant, and M_\star and Ω_\star are the stellar mass and angular velocity respectively.

Table 1: Orbital system initial values

	System 1	System 2	System 3 ¹ A, B	System 4	References
M_*/M_\odot	0.2	0.2	0.2	0.6	
P_*/Days	0.1	0.3	6	10	[24]
$B_{p,*}/\text{G}$	100	50	200	5	[25]
\dot{M}_*/\dot{M}_\odot	0.1	0.1	0.1	1	[26]
m/M_J	[15 - 75]	[15 - 75]	[15 - 75], 75	[2 - 16]	
p_f	6	2.9	0.5, [0.5 - 0.95]	0.5	

¹For system 3 we consider two cases: for case A we change m and fix p_f and for case B, we fix m and change p_f while keeping all the other parameters and system properties unchanged.

1.2 Spin evolution for fully convective stars

The top and bottom panels of Fig. 1 show the time evolution of the rotation period and orbital separation for system 1 of Table 1. For initial values we take a rotation period of $P_* = 0.1$ days, a magnetic field $B_{p,*i} = 100\text{G}$ and orbital separation $a_i = 6R_{co} \approx 0.015\text{AU}$. We consider cases of companion BD masses between $15 - 75M_J$, each represented by a different colour. Black dots are data points from [13] with measured rotation periods, and estimated ages from galactic kinematics for 41 field M-dwarfs. In Fig. 1, the vertical grey dashed lines represent boundaries between thin, intermediate, and thick disk M-dwarf populations with assigned ages $0.5 - 3$ Gyr, $3 - 7$ Gyr, and $7 - 13$ Gyr, respectively. The data points in Fig. 1 use the average value of these disk sub-population ages, since we do not have exact age measurements. The grey area of the top panel corresponds to stellar spin-down without tidal interaction. Solid and dashed lines in the bottom panel correspond to cases with and without tidal interactions respectively. The thickness of the solution curves (grey and coloured) depends on the highest and lowest ϵ values in equation (1), which controls the sharpness of the transition in X-ray luminosity from the saturated (independent of stellar rotation) to the unsaturated (increases with stellar rotation) regimes.

For Fig. 1, the initial orbital separation exceeds the corotation radius. All companions therefore first move outward, gaining angular momentum from the star, and spinning it down faster than the case with only magnetic braking (grey curve). As the star spins down, the corotation radius increases, eventually exceeding the orbital separation and causing the companion to migrate inward.

Comparing the two extreme companion mass cases exemplifies the relative evolution of different mass cases. The heaviest companion (blue curve) extracts angular momentum much faster from the star than the lightest one (red curve), causing a faster inward migration. During the inward migration, the star gains angular momentum from the orbit until the companion is fully tidally shredded, after which spin-down from magnetic braking dominates. In the top panel of Fig. 1, the dips ¹ correspond

¹Double dips result from solving cases with different ϵ values that bound a range in ϵ ; sufficiently different ϵ values give discernibly different engulfment points.

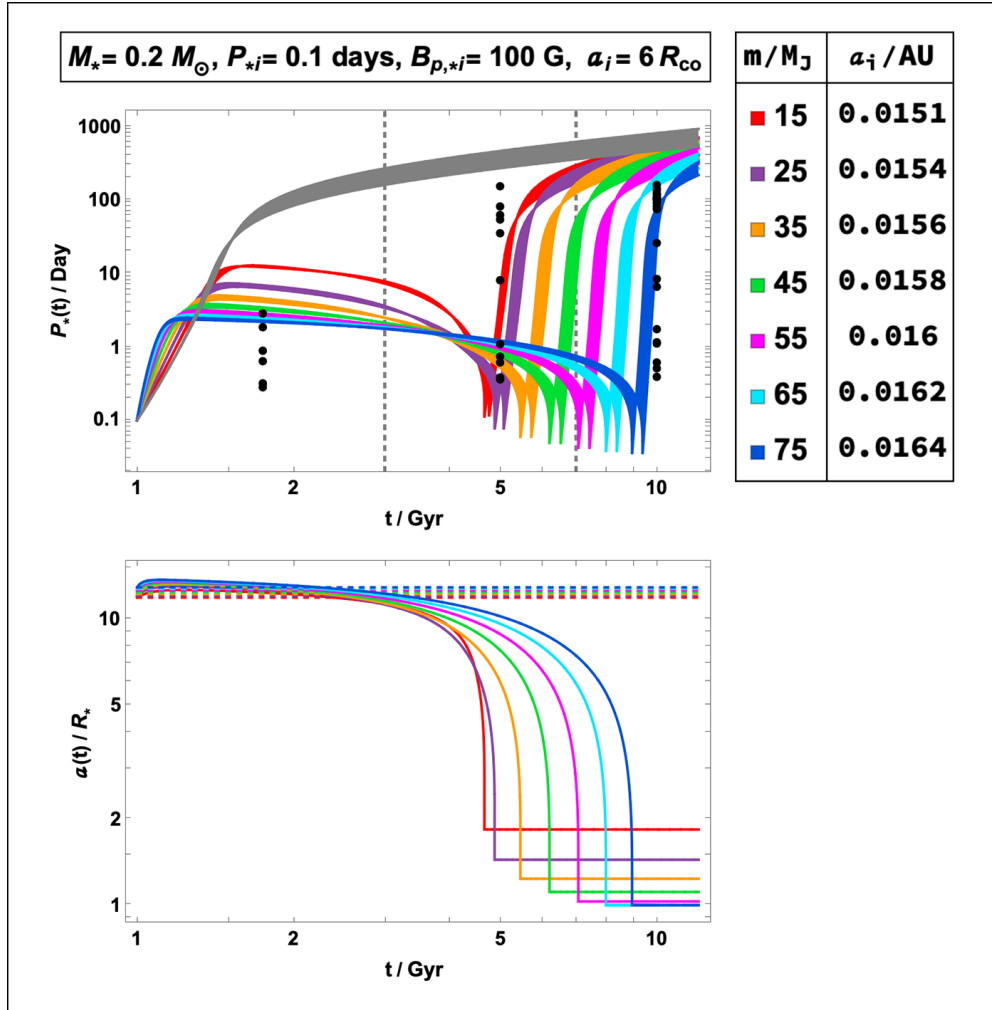


Fig. 1: Evolution of rotation and orbital separation for System 1. We use a $0.2M_\odot$ mass M-dwarf with 0.1 days initial period, 100G magnetic field and companion BD at $a_i = 6R_{\text{co}}$ initial orbital separation. Different colours represent varying BD companion masses between $15 - 75M_J$. Top panel: spin evolution due only to magnetic braking (grey) and coupled to tides (coloured). Cusps represent engulfment points. The thickness of the grey and coloured curves is determined by the highest and lowest ϵ values (see text). Black dots represent fully convective M dwarfs with measured rotation periods and estimated ages from Galactic kinematics [13]. The vertical grey dashed lines separate M-dwarfs in the thin, intermediate and thick disk populations with corresponding age ranges of 0.5 – 3 Gyr, 3 – 7 Gyr and 7 – 13 Gyr. The x-axis and y-axis are normalized to 1 Gyr and a 1-day rotation period, respectively. Bottom panel: orbital separation for solutions without tides (dashed) and coupled to tides (solid) analogous to the top panel. The x-axis is normalized to 1 Gyr, and the y-axis is normalized to the stellar radius R_* .

to the engulfments that occur when the companion reaches the Roche limit or stellar radius, if the latter exceeds the former. In the bottom panel, the flat solid lines correspond to post engulfment evolution.

We find, therefore, that a close BD companion can significantly delay M dwarf spin-down until tidal shredding. Such BD+M-dwarf systems can thus produce old M dwarf populations with short rotation periods. In contrast, without a companion, the stellar wind removes enough angular momentum via magnetic braking to increase the period to hundreds of days. The rapid spin down after BD engulfment can explain the lack of observed M dwarfs with intermediate rotation periods, and thereby explain bimodality in the M dwarf rotation period distribution at a fixed age.

In addition to companion mass and orbital separation, the spin evolution is sensitive to the initial stellar rotation and magnetic field. Given that this combination of quantities are not known for most all M dwarfs yet, we identify values that produce model predictions which capture the bimodal distribution of M dwarfs and fit the data from [13] best. For system 2 in Fig. 2 compared to Fig.1 (system 1), we change the initial rotation period to 0.3 days and decrease the magnetic field to 50G. We keep the same companion mass range and start at $a_i = 2.9R_{\text{co}} \approx 0.015\text{AU}$ initial orbital separation. The spin evolves similarly to the previous case of Fig. 1, but slower. As such, we would not observe tidal shredding of heavier companions within the age of the universe. For companions more massive than $30M_J$, M-dwarf spin-down is delayed and the star remains a fast rotator throughout its MS lifetime. To further illustrate the sensitivity of the spin evolution to the initial magnetic field strength and rotation period, we present complementary cases to the Figs. 1 and Fig. 2 in the supplementary material, varying the initial magnetic field strength and rotation period separately (see Figure S 1 and 2).

For systems 1 and 2, we focused on M-dwarf+BD dynamical evolution for M dwarf initial rotation periods $P_* < 1\text{day}$. In Fig. 3, we show results for system 3A which starts with an M-dwarf of $P_* = 6$ days and $B_{p,*i} = 200\text{G}$, for the same companion BD mass range as in Fig. 2 at the orbital separation of $a_i = 0.5R_{\text{co}}$. Similar to Fig. 1, Fig. 3 shows that the M dwarf initially spins down quickly from magnetic braking, reaching a quasi-equilibrium state $|\gamma_W(t)| \simeq |\gamma_T(t)|$, where $\gamma_W(t)$ and $\gamma_T(t)$ are the dimensionless stellar wind and tidal torque, respectively (equation 17). The companions migrate inward, spinning up the M dwarf but eventually engulfing. The M dwarf subsequently returns to magnetically mediated spin-down. As in Fig. 1, this can explain a rapid spin-down observed for M dwarfs [14]. Here again, not many M-dwarfs would be expected along the steep rising curves on this plot, predicting a bimodality indicated by the two schematically circled regions. However, the bimodality predicted from Fig. 3 would occur over a much shorter age range of only from 7 – 10 Gyr for all companions, compared to that predicted in Fig. 1 and 2.

For system 3B in Fig.4 compared to system 3A of Fig.3, we take the companion mass to be a heavy BD of $75M_J$ to maximize the influence of sub-stellar companion tides, and vary the orbital separation from $a_i = 0.5R_{\text{co}}$ to $a_i = 0.95R_{\text{co}}$. Only when the companion starts at $a_i \leq 0.5R_{\text{co}}$ can it spin up the star before engulfment. Even for heavy BD companions, starting out farther than that cannot prevent the M dwarf from spin-down. Wide enough orbital separations produce mutually similar solution curves.

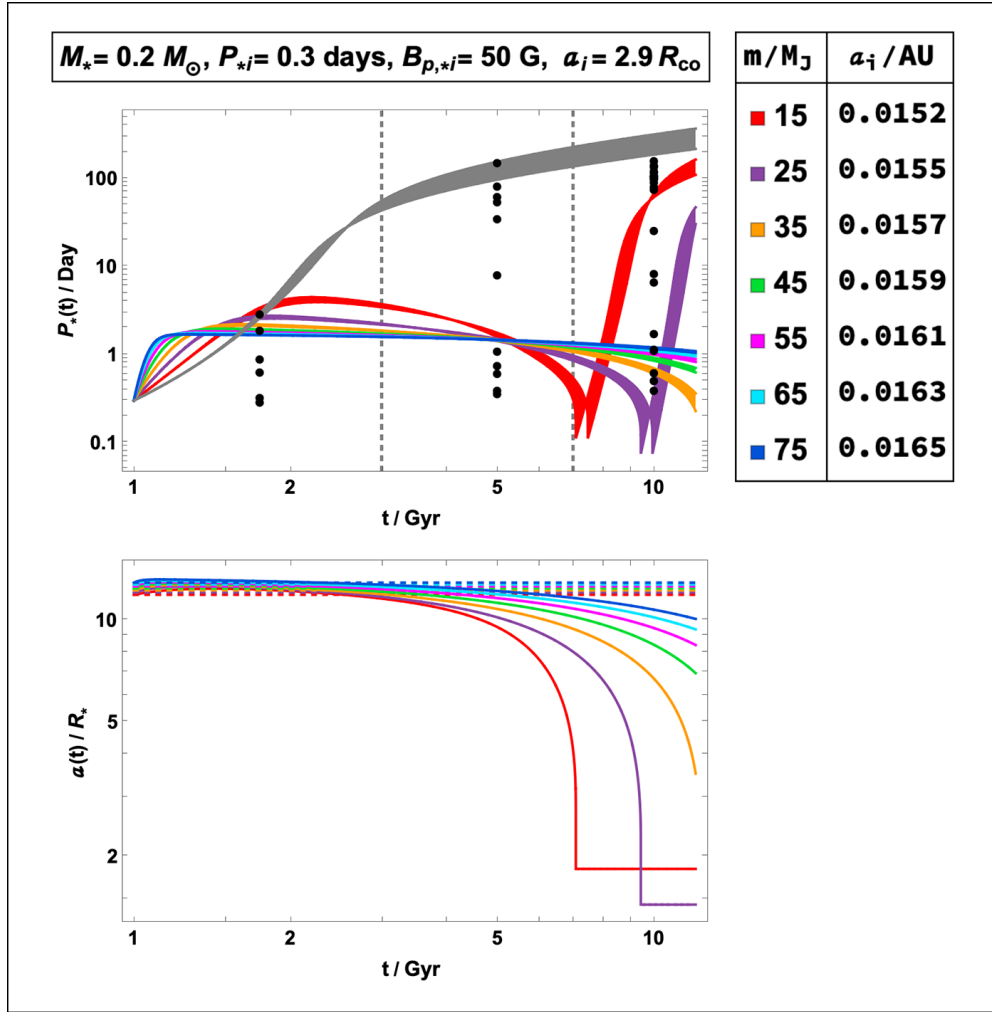


Fig. 2: Evolution of rotation for System 2. We use an M-dwarf with the same stellar and companion BD mass ranges as in Fig. 1, but with initial stellar rotation period of 0.3 days, 50G magnetic field, and orbital separation at $a_i = 2.9R_{co}$. Colours and axes are same as Fig. 1.

Thus a uniform distribution of orbital separations will not produce a uniform spacing of period-age evolution curves. The particular empirical distribution of planet-star orbital separations will produce a distinct signature in the distribution of period-age evolution curves. In turn, a uniform distribution of period-age evolution curves would correspond to a specific non-uniform planet-star orbital separation distribution.

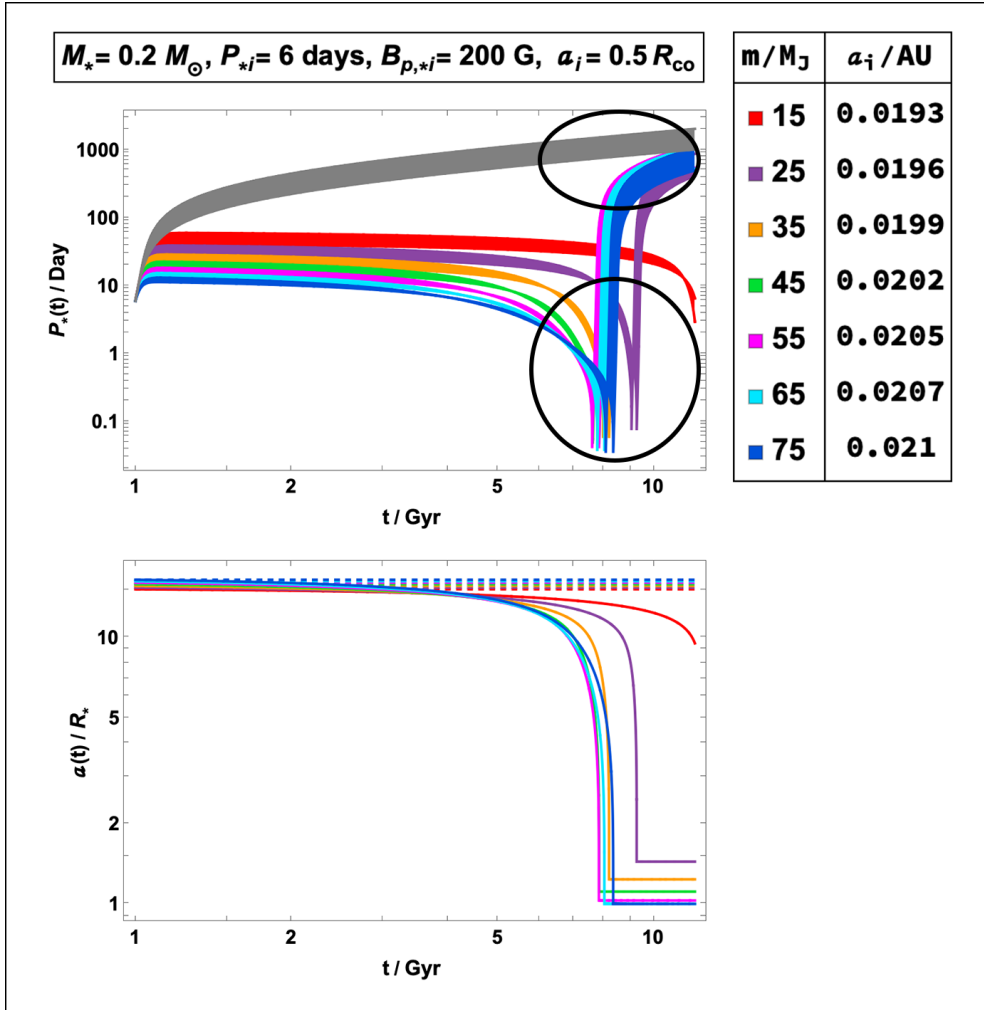


Fig. 3: Evolution of rotation and orbital separation for System 3A. We use an M-dwarf with initial period of 6 days, 200G magnetic field, and orbital separation at $a_i = 0.5R_{\text{co}}$. This causes earlier inward migration of all the companions compared to Fig. 2 but also eventual engulfment. Top panel: black circles qualitatively illustrate the bimodal behaviour of the M-dwarf rotation period during certain ages. Colours and axes are same as Fig. 1.

1.3 Spin evolution for partially convective stars

Jupiter mass companion planets are more common for K-dwarfs than for M-dwarfs. Here we consider system 4 of Table 1, a $0.6M_\odot$ mass star with a 10 day rotation period, 5G magnetic field, and a companion mass range $2M_J \leq m \leq 16M_J$ at an initial orbital separation $a_i = 0.5R_{\text{co}}$. Fig. 5 shows the resulting time evolution of the rotation period

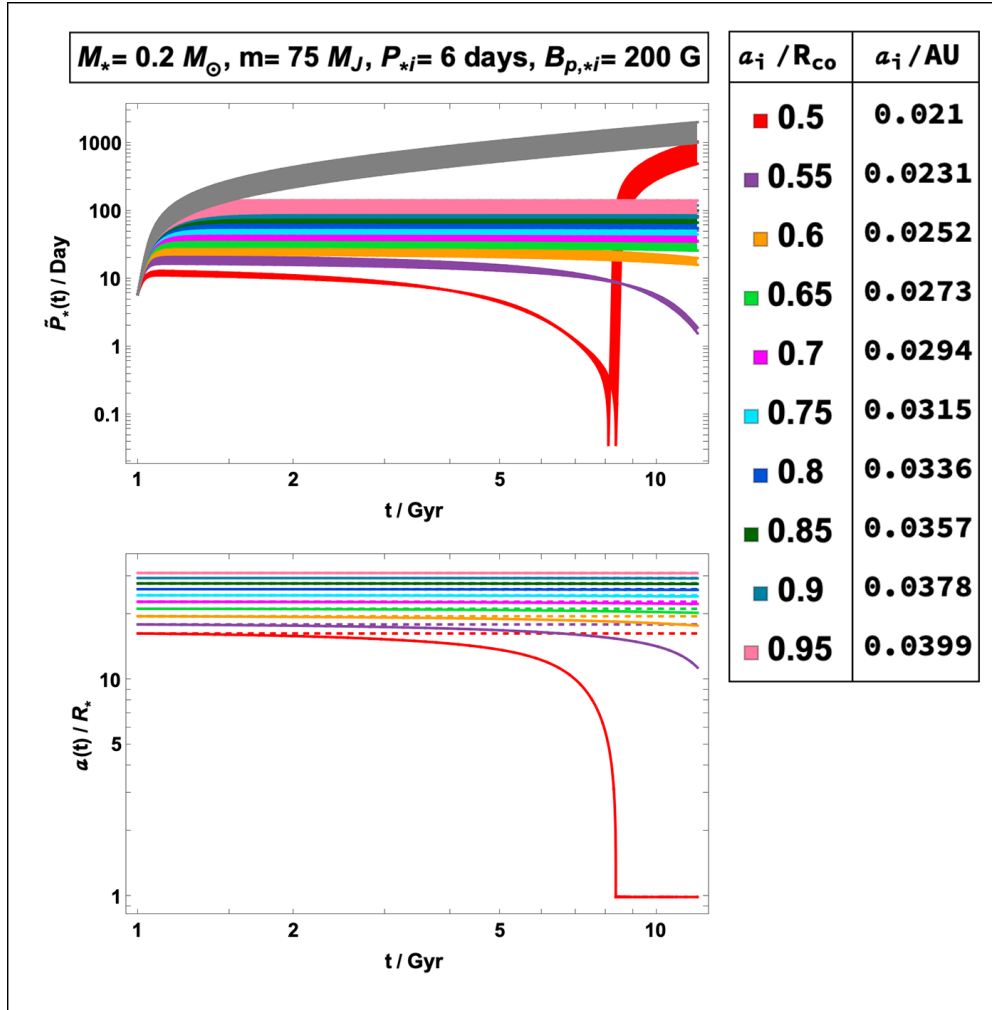


Fig. 4: Evolution of rotation and orbital separation for System 3B. We use an M-dwarf with the same stellar properties as in Fig. 3 and a $m = 75M_J$ companion BD. Here different colours represent different initial orbital separations varying between $0.5 - 0.95R_{co}$. Colours and axes are same as Fig. 1.

and X-ray activity. The plots exemplify that high-mass close companions can spin up a host star (top panel) and thereby increase X-ray activity (bottom panel). Compared to the M-Dwarf+BD systems of Fig. 2, this system produces more evenly distributed curves for a uniform companion mass distribution, so the bimodality discussed for those cases is not predicted here.

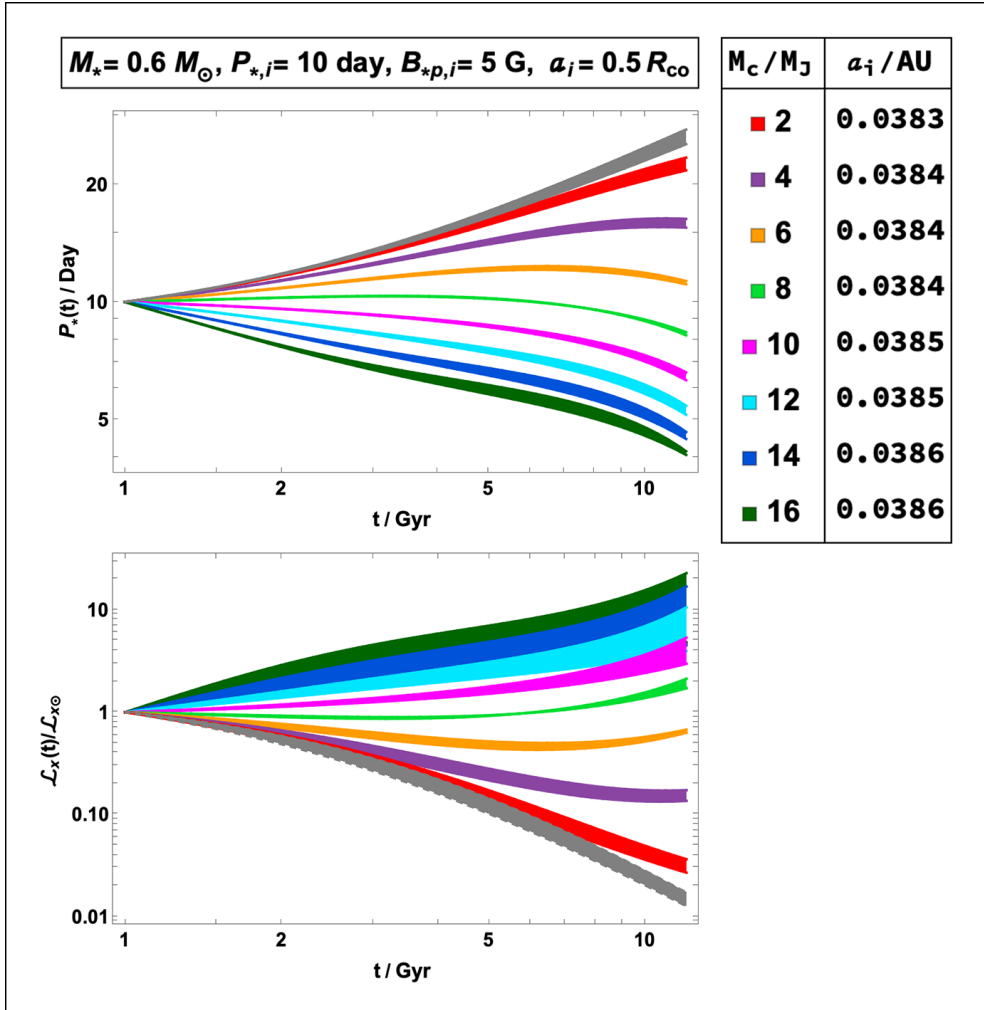


Fig. 5: Evolution of rotation period and X-ray luminosity l_x for System 4. We use a $0.6M_\odot$ mass K-dwarf with a 10 day initial period, 5G magnetic field and an initial orbital separation $a_i = 0.5R_{\text{co}}$. Different colours in each panel represent different companion masses between 2 – 16 M_J . Top panel: colours and axes are the same as Fig. 1. Bottom panel: The x-axis is normalized to 1 Gyr, and the y-axis is normalized to the solar X-ray luminosity $\mathcal{L}_{x\odot}$.

2 Discussion

We have studied the combined influence of tides and magnetic spin-down of M-Dwarfs for different companion BD masses, initial orbital separations, stellar rotations and magnetic field strengths observed. We find that the observed bimodality in period distribution can be reproduced for plausible M-Dwarf+BD systems. Fig. 1, Fig. 2 and Fig.

3 reveal this bimodality in different ways. In Fig. 1, the spin-evolution tracks exhibit a period gap, followed by sharp spin-up spikes during tidal shredding, followed by steeply rising curves that result from the rapid M-dwarf spin-down after companion engulfment. Fig. 2 shows that the spin evolution tracks are separated by a period gap over their full age for most of the companion masses. In Fig. 3 the M-dwarfs initially spin down, but the companions move inward fast enough to then rapidly spin-up the star, consistent with an observational period gap [11, 13, 14]. After companions are engulfed, the stars rapidly spin down by magnetic braking. Since the spin-down transition regime is so short, the fraction of stars therein is small and the overall period distributions becomes approximately bimodal. We have included only equilibrium tides in this work. Dynamical tides can enhance the tidal influence and offset the spindown of even more magnetically active M-dwarfs than we have considered. This would be particularly important for modeling a specific M dwarf-BD system, were data to become available. Future work can extend our present calculations.

For a $0.6M_{\odot}$ partially convective star, Fig. 5 shows that a uniform distribution of companion masses produces more evenly spaced curves than the more pronounced bimodal distribution for fully convective M dwarf cases of Figs. 1, 2 and 3. This is independent of any magnetic topology changes or changes in core to envelope magnetic coupling which have elsewhere been proposed to influence spin evolution [27, 28]. In our framework, the absence of bimodality for partially convective stars compared to fully convective M-dwarfs would reveal differences in companion mass and orbital separation distributions between the two stellar population classes. This, in turn, would provide indirect constraints on the statistics of stellar-planetary system formation outcomes. In fact, observations do show that lower mass M dwarfs have a higher companion to primary mass ratio m/M_{\star} , that increases exponentially with decreasing mass for M-dwarfs of masses $M_{\star} \lesssim 0.25M_{\odot}$. In addition, massive M-dwarfs of $M_{\star} \gtrsim 0.35M_{\odot}$ lack companions at very close separations [29]. These trends would imply statistically larger tidal torques and a more pronounced bimodal period distribution for fully convective M-dwarfs (see equation (10)), and relative to their partially convective counterparts.

There is a degeneracy between companion mass and orbital separation in our model if we do not know either. Knowing either from observations for a specific system can eliminate this degeneracy. Also, the predicted spin evolution is more sensitive to orbital separation than to companion mass and so observations that pin down the orbital separation distributions will help to constrain the predicted fraction of M-dwarfs whose spin is tidally influenced by companions. For example, a uniform distribution of companion separations could imply that in $\sim 80\%$ of systems the companion would not influence spin substantially (Fig. 4) whilst a higher fraction of companions at smaller separations would exacerbate the relative population of old M-dwarfs with anomalously short periods. Complementarily, the observed spin bimodality for old M-dwarfs can be used to constrain BD or planet mass-orbital separation distributions around fully convective M dwarfs. If tides are the reason for the bimodality, this would help to predict the presence of BD companions and prioritize particular systems for companion searches in follow-up observations.

Gyrochronology can in principle determine isolated low-mass MS stellar ages with reasonable precision [30]. But our study shows how the one-to-one mapping on which

this method depends is broken with companions. Moreover, although we have explored scenarios with just one companion, the occurrence rate of planets around M dwarfs is at least 3.0 planets per star, potentially exacerbating the influence of tides on spin [31] and age-rotation degeneracy. Recalibrating gyrochronology to account for tides would be desirable to extend its utility beyond isolated stars. This is challenging but maybe possible because, for a large range of companion BD masses over a large age range, the period evolves little (see Fig. 2). Also, the curves for heavier companions are close together, and less sensitive to the influence of a specific companion mass.

Finally, although observations show no sharp weakening of the rotation-activity at the fully convective M dwarf boundary (around M3 spectral type) they do show a sharp drop in activity for stars later than spectral type M8 [32, 33]. [33] suggested that magnetic braking is less effective in stars later than M8 because the low ionization fraction leads to a high enough magnetic diffusivity such that the magnetic field decouples from the plasma near the surface. This implies a correlation between low activity and short spin periods in these M-dwarfs that is also consistent with our calculations as tides do little to exacerbate spin down for these cases. We would therefore predict that observations will not reveal a significant population of long period low mass M-dwarfs later than M8, unless magnetic braking can somehow survive even in stars with very low ionization layers.

3 Methods

3.1 Magnetic spin-down model for an isolated magnetized star

In our theoretical spin evolution model that dynamically couples stellar spin, magnetic field strength, X-ray luminosity and mass loss, dynamo-generated magnetic fields are the main coronal energy source supplying both open and closed coronal fields. Hot gas propagates along open field lines and removes angular momentum, while magnetic dissipation of closed, field lines sources X-ray emission. More detailed derivations are in [23] where the original model was applied to the Sun, and it was further developed in [34] and applied to older-than-solar low-mass MS stars. The main ingredients are an isothermal Parker wind [35]; angular momentum loss from the equatorial plane [36]; a dynamo saturation prescription based on a combination of magnetic helicity evolution and buoyant loss of magnetic fields [37, 38], used to estimate the magnetic field strength; replacement of the convection time in the dynamo coefficients by shear or rotation time for fast rotators [39]; and a coronal equilibrium condition [40] that determines how the magnetic energy supply is distributed into radiation, wind, and conductive losses. Together, these components lead to a system of coupled equations for the X-ray luminosity, magnetic field, spin evolution and mass loss below.

The first necessary equation is the relation between X-ray luminosity $l_{x\star}(t)$ and radial magnetic field $b_{r\star}(t)$:

$$l_{x\star}(t) \equiv g_L(t) \left(\frac{\text{erf}(\epsilon/\tilde{R}o_\star)}{\text{erf}(\epsilon/\tilde{R}o(t))} \right)^{\frac{4}{3(1-\lambda)}} \left(\frac{1 + \tilde{R}o_\star/\text{erf}(\epsilon/\tilde{R}o_\star)}{1 + \tilde{R}o(t)/\text{erf}(\epsilon/\tilde{R}o(t))} \right)^{\frac{2}{1-\lambda}} = b_{r\star}(t)^{\frac{4}{1-\lambda}}. \quad (1)$$

Compared to the original model of [23], here we have generalized the prescription for the correlation timescale. Instead of using a shear parameter we use the error function $\text{erf}(\epsilon/\tilde{R}o_\star)$ which depends on the a parameter ϵ and Rossby number $\tilde{R}o_\star$. Here λ represents the power law of the dependence of magnetic starspot area covering fraction on X-ray luminosity. More details on the numerical values of paramters used are in section 3.4. We assume $g_L(t) \approx 1$, which measures the bolometric luminosity evolution on the main sequence for both partially and fully convective stars.

Next we have the equation for the toroidal magnetic field:

$$b_{\phi\star}(t) \equiv \frac{B_{\phi\star}(t)}{B_{\phi,\star i}} = -\frac{\dot{m}_\star(t)\omega_\star(t)}{b_{r_\star}(t)} \frac{M_\star\Omega_{\star i}}{R_\star B_{\phi,\star i} B_{r,\star i}} \left[\frac{r_A(t)^2}{R_\star^2} - 1 \right], \quad (2)$$

where $b_{\phi\star}(t)$ is the dimensionless toroidal magnetic field, normalized to the initial toroidal magnetic field $B_{\phi,\star i}$ ². Quantities $\dot{M}_{\star i}$, $B_{r,\star i}$, $\Omega_{\star i}$ are initial mass loss, radial magnetic field, and angular velocity, respectively; $\dot{m}_\star(t)$ is a mass loss rate (see equations 4 and 5 below); M_\star and R_\star are the stellar mass and radius, assumed to be constant; the Alfvén radius r_A is given below in equation (6); $\omega_\star(t) = \Omega_\star(t)/\Omega_{\star i}$ is the dimensionless angular velocity described by

$$\frac{d\omega_\star(t)}{d\tau} = -\omega_\star(t)t_\star \frac{q}{\beta_\star^2} \frac{b_{r\star}(t)^2}{m_\star \tilde{u}_A(t)} \frac{B_{r,\star i}^2 R_\star^2}{M_\star u_{A,\star i}}, \quad (3)$$

where t_\star is the normalization parameter taken as 1 Gyr. Here β_\star is the radius of gyration; q is a dimensionless moment of inertia parameter that depends on the assumed constant fraction of the star in which the field is anchored; $\tilde{u}_A(t)$ and $u_{A,\star i}$ are the dimensionless Alfvén speed and initial value for Alfvén speed; and $m_\star = 1$ is the dimensionless stellar mass in units of initial stellar mass, which does not evolve.

The fourth equation needed for the model is the mass loss rate, for which we have two regimes. For the thermal conduction loss dominated regime - Regime I:

$$\dot{m}_\star(t) \simeq l_{x\star}(t)^{\frac{23}{38}} \exp \left[\frac{3.9}{\tilde{T}_{0\star}} \frac{m_{\odot\star}}{r_{\odot\star}} \left(1 - (l_{x\star}(t))^{-\frac{16}{9}} \right) \right], \quad (4)$$

whilst for the wind loss dominated regime - Regime II:

$$\dot{m}_\star(t) \simeq l_{x\star}(t) \simeq \exp \left[\ln(\tilde{T}_{0\star}) + \frac{7.8}{\tilde{T}_{0\star}} \frac{m_{\odot\star}}{r_{\odot\star}} \left(\frac{\tilde{T}_{0\star}}{\tilde{T}_{0,\star i}} - 1 \right) \right], \quad (5)$$

where $\tilde{T}_{0\star}(t)$ is a dimensionless coronal temperature at equilibrium, normalized such that transition between regime I and regime II occurs at $\tilde{T}_{0\star} = 0.5$. The $\tilde{T}_{0,\star i}$ represents the initial coronal temperature.³ Here $m_{\odot\star} = \frac{M_\star}{M_\odot}$ and $r_{\odot\star} = \frac{R_0}{R_\odot} \sim \frac{R_\star}{R_\odot}$, where R_0 represents radius at the coronal base; M_\odot and R_\odot are solar mass and radius respectively.

²We substitute subscript i for n used in [23], as here we use initial stellar values for rather than present-day values.

³Here we have included the correction [41] to [34].

The Alfvén radius needed for equation (2) and derived following [23, 36, 42] is

$$\frac{r_A(t)}{R_\star} = \frac{b_{r_\star}(t)}{\dot{m}_\star(t)^{1/2} \tilde{u}_A(t)^{1/2}} \frac{R_\star B_{r,\star i}}{\dot{M}_{\star i}^{1/2} u_{A,\star i}^{1/2}}, \quad (6)$$

where the Alfvén speed is given by

$$\tilde{u}_A(t) \equiv \frac{u_A(t)}{u_{A,\star i}} = \sqrt{\frac{T_{0\star}(t)}{T_{0,\star b}} \frac{W_h[-D(r_A(t))]}{W_h[-D(r_{A,\star i})]}}, \quad (7)$$

where $W_h[-D(r_A)]$ is the Lambert W function for the Parker wind with $h = 0$ for $r \leq r_s$ and $h = -1$ for $r \geq r_s$ [43], and

$$D(r_A) = \left(\frac{r_A}{r_s}\right)^{-4} \exp\left[4\left(1 - \frac{r_s}{r_A}\right) - 1\right]. \quad (8)$$

where the sonic radius is given by

$$\frac{r_s}{R_\star} = \frac{GM_\star}{2c_s^2 R_\star} \quad (9)$$

with isothermal sound speed c_s .

3.2 Influence of tides on the evolution of stellar spin

The spin evolution model summarized in the previous section must be generalized to account for tidal stresses, which can exchange angular momentum between the orbit and the spins of the primary and secondary when the primary star has a close stellar or sub-stellar companion. We assume that tidal stresses are redistributed much faster than the secular spin evolution that we will solve for [44, 45]. We focus only on equilibrium tides, for which the star evolves in hydrostatic equilibrium during its response to tidal forcing (e.g, [16, 46]).

We consider a sub-stellar companion in a circular orbit, and a uniform rotation of the primary star at angular velocity Ω_\star . The gravitational field of the secondary deforms the primary, and vice-versa but we focus on the former. Since the star is not a perfect fluid, it will incur a viscously mediated time lag Δt to the deformation that offsets the direction of tidal bulges from the instantaneous direction of the external force by a small angle δ , producing a torque. In the weak-friction approximation $\delta \ll 1$, the tidal torque Γ_T on the primary can be written (e.g [46]):

$$\Gamma_T \simeq -3k \frac{Gm^2}{R_\star} \left(\frac{R_\star}{a}\right)^6 \delta, \quad (10)$$

where m is the secondary (companion) mass and a is the orbital separation. Here k is the apsidal motion constant determined by the structure of the star.

In the weak friction approximation,

$$\delta = (\Omega_\star - \Omega_{\text{orb}})\Delta t = (\Omega_\star - \Omega_{\text{orb}})\frac{t_{\text{ff}}^2}{t_{\text{diss}}}, \quad (11)$$

showing that δ is linearly proportional to the departure from synchronism and a constant factor $\Delta t = t_{\text{ff}}^2/t_{\text{diss}}$, the ratio of the free-fall time squared to a dissipation time. Here $t_{\text{ff}} = (GM_\star/R_\star^3)^{-1/2}$ with orbital angular velocity Ω_{orb} given by:

$$\Omega_{\text{orb}} = \left[\frac{G(M_\star + m)}{a^3} \right]^{1/2}. \quad (12)$$

The time t_{ff} is determined by the time scale for kinetic energy dissipation in the stellar convection zone and can be written $t_{\text{diss}} = R^2/\nu_t \simeq (M_\star R_\star^2/L_\star)^{1/3}$ [46], where ν_t is eddy viscosity and L_\star is the stellar bolometric luminosity.

Combining equations (10) and (11) gives the evolution of stellar angular velocity due to tides:

$$\Gamma_{\text{T}} = I_\star \left. \frac{d\Omega_\star}{dt} \right|_{\text{T}} = -3k \frac{(\Omega_\star - \Omega_{\text{orb}})}{t_{\text{diss}}} \left(\frac{m}{M_\star} \right)^2 M_\star R_\star^2 \left(\frac{R_\star}{a} \right)^6, \quad (13)$$

where I_\star is the moment of inertia of the star. Equation (13) shows that only when the stellar rotation is unsynchronized with the orbital motion so that $\Omega_\star \neq \Omega_{\text{orb}}$, does a finite t_{diss} cause a lag of the tidal bulges $\delta \neq 0$, and in turn, a tidal torque.

From conservation of total angular momentum of the star and companion, considering only tidal interaction without magnetic braking, $d[I_\star\Omega_\star(t) + ma^2(t)\Omega_{\text{orb}}(t)]/dt = 0$ and correspondingly, the evolution of orbital separation is

$$\frac{da(t)}{dt} = -a(t)^{1/2}\Gamma_{\text{T}}(t)\frac{2}{m(G(M_\star + m))^{1/2}}, \quad (14)$$

which can be rewritten in dimensionless form as

$$\frac{d\tilde{a}(t)}{d\tau} = -\tilde{a}(t)^{1/2}\gamma_{\text{T}}(t)\frac{2\beta_\star^2 M_\star}{q m} \left(\frac{\chi M_\star}{M_\star + m} \right)^{1/2}, \quad (15)$$

where $\gamma_{\text{T}} = \left. \frac{d\omega_\star}{d\tau} \right|_{\text{T}} = \Gamma_{\text{T}}t_\star/I_\star\Omega_\star$ is the dimensionless tidal torque and $\chi = \Omega_\star^2 R_\star^3/GM_\star$ is a dimensionless ratio of stellar rotation speed to the Keplerian speed at its surface. The equation for the tidal torque in dimensionless form can then be written

$$\gamma_{\text{T}}(t) = -3k \frac{t_\star}{t_{\text{diss}}} \frac{q}{\beta_\star^2} \left(\omega_\star(t) - \left(\frac{r_\star}{\tilde{a}(t)} \right)^{3/2} \left(\frac{M_\star + m}{\chi M_\star} \right) \right) \left(\frac{m}{M_\star} \right)^2 \left(\frac{r_\star}{\tilde{a}(t)} \right)^6. \quad (16)$$

where we have used equation (12) to eliminate Ω_{orb} from equation (13) and rewritten it in terms of orbital separation $a(t)$.

3.3 Combining magnetic braking and tides

Using a similar dimensionless prescription for the magnetic braking-induced wind torque as used for tides, we have $\gamma_W = \frac{d\omega_\star}{d\tau}|_W = \Gamma_W t_\star / I_\star \Omega_\star$ and the generalized equation for stellar spin evolution that combines both torques can be written as

$$\begin{aligned} \frac{d\omega_\star(t)}{d\tau} &= \gamma_W(t) + \gamma_T(t)(1 - 2H(\tilde{a}_{\text{crit}} - \tilde{a}(t))) \\ &= -\omega_\star(t)t_\star \frac{q}{\beta_\star^2} \frac{b_{r_\star}(t)^2}{m_\star \tilde{u}_A(t)} \frac{B_{r_\star, \star i}^2 R_\star^2}{M_{\star i} u_{A, \star i}} \\ &\quad - 3k \frac{t_\star}{t_{\text{diss}}} \frac{q}{\beta_\star^2} \left(\omega_\star(t) - \left(\frac{r_\star}{\tilde{a}(t)} \right)^{3/2} \left(\frac{M_\star + m}{\chi M_\star} \right) \right) \left(\frac{m}{M_\star} \right)^2 \left(\frac{r_\star}{\tilde{a}(t)} \right)^6 \times \\ &\quad \times (1 - 2H(\tilde{a}_{\text{crit}} - \tilde{a}(t))). \end{aligned} \quad (17)$$

To account for the demise of the companion when it reaches the larger of the Roche limit or stellar radius, we include a multiplicative function $(1 - 2H(\tilde{a}_{\text{crit}} - \tilde{a}(t)))$ in the tidal torque term, where $H(\tilde{a}_{\text{crit}} - \tilde{a}(t))$ is the logistic function given by

$$H(\tilde{a}_{\text{crit}} - \tilde{a}(t)) = \frac{1}{1 + \exp[-0.2(\tilde{a}_{\text{crit}} - \tilde{a}(t))]} \quad (18)$$

While the magnetic braking term always decreases the stellar spin, the influence of the tidal term depends on the orbital evolution of the secondary. If the secondary moves outward, then the orbital angular momentum will increase and tidal force will act to spin down the star. But if the secondary moves inward, reducing the orbital angular momentum, then tides increase the stellar spin. This evolution is thought to be much more efficient for cool stars with outer convection zones than for hot stars with outer radiative layers [44].

For sufficient inward migration, planet engulfment may occur [e.g. 47, 48], accompanied by an increase in the stellar rotation [47, 49]. Depending on stellar and companion properties, there may also be an accompanying rapid increase in luminosity [47] and change in the surface abundance of lithium [49].

3.4 Fixed model parameters

To solve for the stellar spin evolution from the system of equations (1), (2), (4) (5), (7), (15) and (17) (or (3) replacing (17) when only magnetic braking is considered) there are several parameters that we keep fixed for all of the cases that we solve: (i) We take $0.009 \leq \epsilon \leq 0.0036$ which is consistent with model-inferred Rossby numbers for the transition to the X-ray saturated regime of both partially and fully convective stars [1, 50, 51] and the range accounts for the corresponding uncertainty in the saturation Rossby number. (ii) we take $\lambda = 1/3$, consistent with the range inferred from observations of star spot covering fractions for FGKM stars [52]. (iii) We use $q = 1$ for all stars, which is equivalent to assuming that the full stellar mass is coupled to the anchoring magnetic field that contributes to spin-down. (iv) For the radius of gyration

β_* and apsidal motion constant k , we use values from stellar evolutionary models, where the evolutionary tracks are computed using the Modules for Experiments in Stellar Astrophysics package (MESA) [53]. (vi) For the convective turnover timescale τ_c we use the prescription given in [51].

Supplementary information. This article has accompanying supplementary information.

Acknowledgments. KK acknowledges support from a Horton Graduate Fellowship from the Laboratory for Laser Energetics. We acknowledge support from National Science Foundation grant PHY-2020249. EB acknowledges the Isaac Newton Institute for Mathematical Sciences, Cambridge, for support and hospitality during the programme "Frontiers in dynamo theory: from the Earth to the stars", supported by EPSRC grant no EP/R014604/1.

Declarations

Some journals require declarations to be submitted in a standardised format. Please check the Instructions for Authors of the journal to which you are submitting to see if you need to complete this section. If yes, your manuscript must contain the following sections under the heading 'Declarations':

- Funding: see **Acknowledgments**
- Conflict of interest/Competing interests (check journal-specific guidelines for which heading to use). The authors have no conflicts of interest.
- Ethics approval Not applicable
- Consent to participate Not applicable
- Consent for publication Not applicable
- Availability of data and materials Not applicable
- Code availability Not applicable
- Authors' contributions Both authors contributed equally to the writing of the manuscript, discussions, and analysis of the results. K.K. also carried out the calculations and prepared the figures.

References

- [1] Wright, N.J., Drake, J.J., Mamajek, E.E., Henry, G.W.: The Stellar-activity-Rotation Relationship and the Evolution of Stellar Dynamos. *ApJ* **743**, 48 (2011) <https://doi.org/10.1088/0004-637X/743/1/48> arXiv:1109.4634 [astro-ph.SR]
- [2] Reiners, A., Mohanty, S.: Radius-dependent Angular Momentum Evolution in Low-mass Stars. I. *ApJ* **746**, 43 (2012) <https://doi.org/10.1088/0004-637X/746/1/43> arXiv:1111.7071 [astro-ph.SR]
- [3] Meibom, S., Mathieu, R.D., Stassun, K.G.: Stellar rotation in m35: Mass-period relations, spin-down rates, and gyrochronology. *The Astrophysical Journal* **695**(1), 679 (2009)

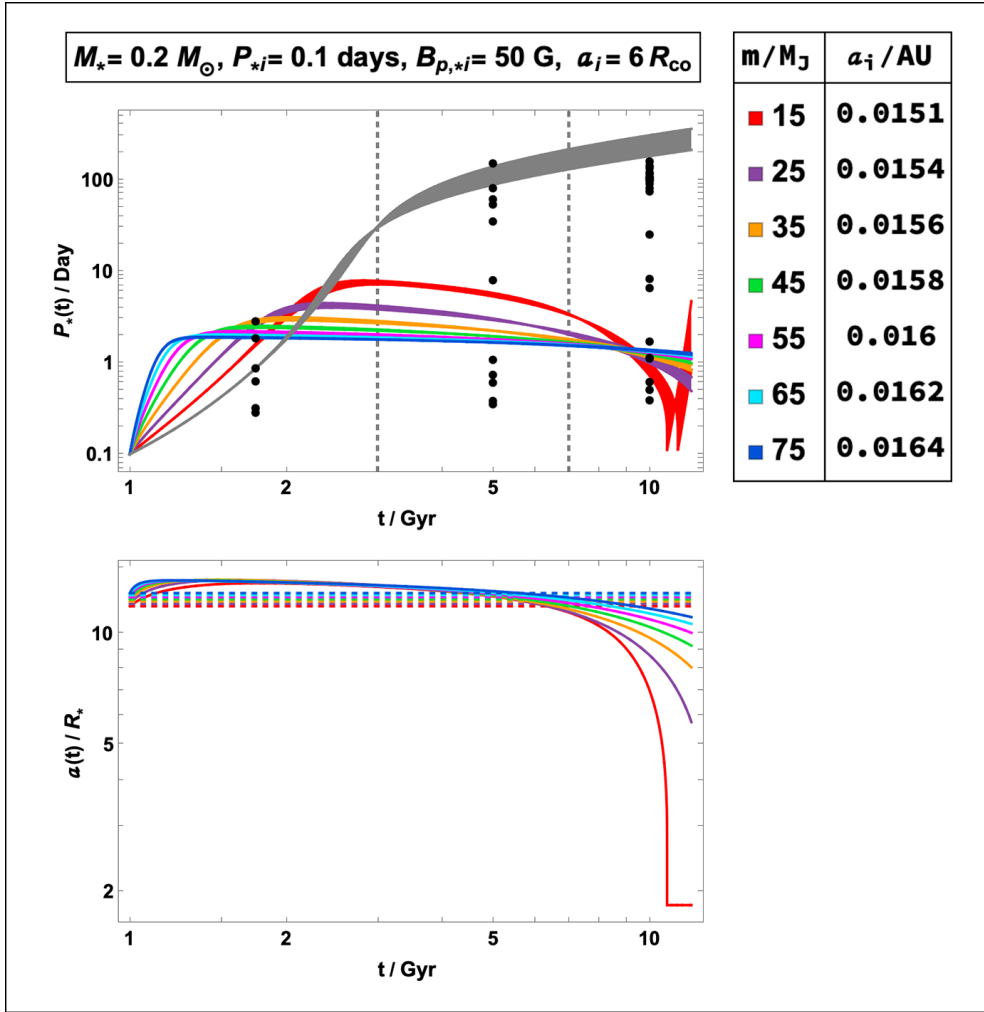


Figure S 1: M-dwarf with the same initial properties and companion BDs as in Fig. 1, but with an initial 50G magnetic field. Colours and axes are the same as Fig. 1.

- [4] Meibom, S., Barnes, S.A., Latham, D.W., Batalha, N., Borucki, W.J., Koch, D.G., Basri, G., Walkowicz, L.M., Janes, K.A., Jenkins, J., *et al.*: The kepler cluster study: Stellar rotation in ngc 6811. *The Astrophysical Journal Letters* **733**(1), 9 (2011)
- [5] Agüeros, M., Bowsher, E., Bochanski, J., Cargile, P., Covey, K., Douglas, S., Kraus, A., Kundert, A., Law, N., Ahmadi, A., *et al.*: A new look at an old cluster: The membership, rotation, and magnetic activity of low-mass stars in the 1.3 kyr old open cluster ngc 752. *The Astrophysical Journal* **862**(1), 33 (2018)

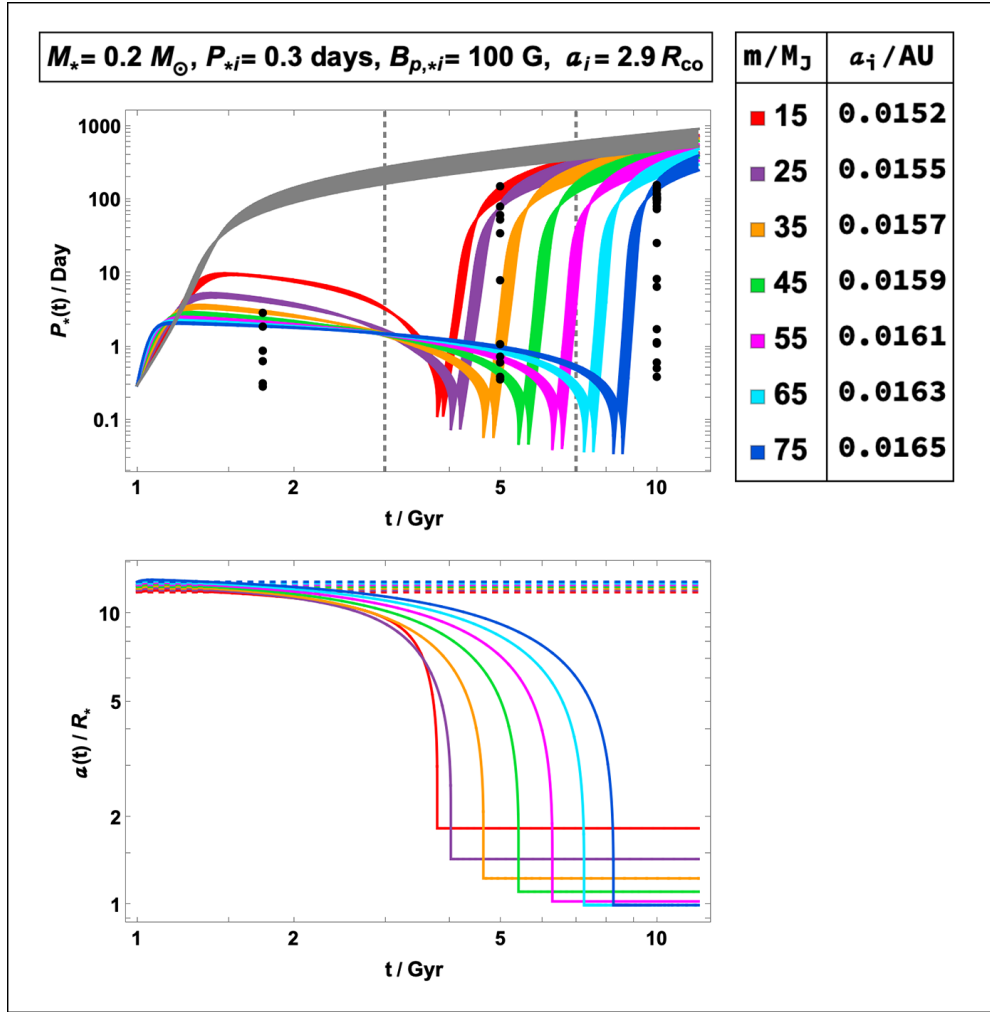


Figure S 2: M-dwarf with the same properties and companion BDs as in Fig. 2, but with initial 100G magnetic field strength. Everything else is illustrated and normalized similar to Fig. 2.

- [6] Matt, S.P., MacGregor, K.B., Pinsonneault, M.H., Greene, T.P.: Magnetic Braking Formulation for Sun-like Stars: Dependence on Dipole Field Strength and Rotation Rate. *ApJ* **754**, 26 (2012) <https://doi.org/10.1088/2041-8205/754/2/L26> [arXiv:1206.2354](https://arxiv.org/abs/1206.2354) [astro-ph.SR]
- [7] van Saders, J.L., Pinsonneault, M.H.: Fast Star, Slow Star; Old Star, Young Star: Subgiant Rotation as a Population and Stellar Physics Diagnostic. *ApJ* **776**, 67 (2013) <https://doi.org/10.1088/0004-637X/776/2/67> [arXiv:1306.3701](https://arxiv.org/abs/1306.3701) [astro-ph.SR]

- [8] Gallet, F., Bouvier, J.: Improved angular momentum evolution model for solar-like stars. *Astronomy & Astrophysics* **556**, 36 (2013)
- [9] Matt, S.P., Brun, A.S., Baraffe, I., Bouvier, J., Chabrier, G.: The Mass-dependence of Angular Momentum Evolution in Sun-like Stars. *ApJ* **799**, 23 (2015) <https://doi.org/10.1088/2041-8205/799/2/L23> arXiv:1412.4786 [astro-ph.SR]
- [10] van Saders, J.L., Ceillier, T., Metcalfe, T.S., Silva Aguirre, V., Pinsonneault, M.H., García, R.A., Mathur, S., Davies, G.R.: Weakened magnetic braking as the origin of anomalously rapid rotation in old field stars. *Nature* **529**, 181–184 (2016) arXiv:1601.02631 [astro-ph.SR]
- [11] McQuillan, A., Mazeh, T., Aigrain, S.: Stellar Rotation Periods of the Kepler Objects of Interest: A Dearth of Close-in Planets around Fast Rotators. *ApJ* **775**(1), 11 (2013) <https://doi.org/10.1088/2041-8205/775/1/L11> arXiv:1308.1845 [astro-ph.EP]
- [12] Rebull, L.M., Stauffer, J.R., Bouvier, J., Cody, A.M., Hillenbrand, L.A., Soderblom, D.R., Valenti, J., Barrado, D., Bouy, H., Ciardi, D., Pinsonneault, M., Stassun, K., Micela, G., Aigrain, S., Vrba, F., Somers, G., Christiansen, J., Gillen, E., Cameron, A.C.: Rotation in the pleiades with k2. i. data and first results. *The Astronomical Journal* **152**(5), 113 (2016) <https://doi.org/10.3847/0004-6256/152/5/113>
- [13] Irwin, J., Berta, Z.K., Burke, C.J., Charbonneau, D., Nutzman, P., West, A.A., Falco, E.E.: On the angular momentum evolution of fully convective stars: rotation periods for field m-dwarfs from the nearth transit survey. *The Astrophysical Journal* **727**(1), 56 (2011)
- [14] Newton, E.R., Irwin, J., Charbonneau, D., Berta-Thompson, Z.K., Dittmann, J.A., West, A.A.: The Rotation and Galactic Kinematics of Mid M Dwarfs in the Solar Neighborhood. *ApJ* **821**(2), 93 (2016) <https://doi.org/10.3847/0004-637X/821/2/93> arXiv:1511.00957 [astro-ph.SR]
- [15] Metcalfe, T.S., Egeland, R., van Saders, J.: Stellar Evidence That the Solar Dynamo May Be in Transition. *ApJ* **826**(1), 2 (2016) <https://doi.org/10.3847/2041-8205/826/1/L2> arXiv:1606.01926 [astro-ph.SR]
- [16] Zahn, J.-P.: Tidal friction in close binary systems. *A&A* **57**, 383–394 (1977)
- [17] Ogilvie, G.I., Lin, D.N.C.: Tidal Dissipation in Rotating Solar-Type Stars. *ApJ* **661**(2), 1180–1191 (2007) <https://doi.org/10.1086/515435> arXiv:astro-ph/0702492 [astro-ph]
- [18] Ogilvie, G.I.: Tides in rotating barotropic fluid bodies: the contribution of inertial waves and the role of internal structure. *MNRAS* **429**(1), 613–632 (2013) <https://doi.org/10.1093/mnras/stt100>

[//doi.org/10.1093/mnras/sts362](https://doi.org/10.1093/mnras/sts362) arXiv:1211.0837 [astro-ph.EP]

- [19] Mathis, S.: Variation of tidal dissipation in the convective envelope of low-mass stars along their evolution. *A&A* **580**, 3 (2015) <https://doi.org/10.1051/0004-6361/201526472> arXiv:1507.00165 [astro-ph.SR]
- [20] Gallet, F., Bouvier, J.: Improved angular momentum evolution model for solar-like stars. *A&A* **556**, 36 (2013) <https://doi.org/10.1051/0004-6361/201321302> arXiv:1306.2130 [astro-ph.SR]
- [21] Gallet, F., Bouvier, J.: Improved angular momentum evolution model for solar-like stars. II. Exploring the mass dependence. *A&A* **577**, 98 (2015) <https://doi.org/10.1051/0004-6361/201525660> arXiv:1502.05801 [astro-ph.SR]
- [22] Amard, L., Palacios, A., Charbonnel, C., Gallet, F., Bouvier, J.: Rotating models of young solar-type stars. Exploring braking laws and angular momentum transport processes. *A&A* **587**, 105 (2016) <https://doi.org/10.1051/0004-6361/201527349> arXiv:1601.01904 [astro-ph.SR]
- [23] Blackman, E.G., Owen, J.E.: Minimalist coupled evolution model for stellar X-ray activity, rotation, mass loss, and magnetic field. *MNRAS* **458**, 1548–1558 (2016) <https://doi.org/10.1093/mnras/stw369> arXiv:1511.05658 [astro-ph.SR]
- [24] Popinchalk, M., Faherty, J.K., Kiman, R., Gagné, J., Curtis, J.L., Angus, R., Cruz, K.L., Rice, E.L.: Evaluating rotation periods of m dwarfs across the ages. *The Astrophysical Journal* **916**(2), 77 (2021)
- [25] Kochukhov, O.: Magnetic fields of m dwarfs. *The Astronomy and Astrophysics Review* **29**(1) (2020) <https://doi.org/10.1007/s00159-020-00130-3>
- [26] Wood, B.E., Müller, H.-R., Redfield, S., Konow, F., Vannier, H., Linsky, J.L., Youngblood, A., Vidotto, A.A., Jardine, M., Alvarado-Gómez, J.D., Drake, J.J.: New Observational Constraints on the Winds of M dwarf Stars. *ApJ* **915**(1), 37 (2021) <https://doi.org/10.3847/1538-4357/abfda5> arXiv:2105.00019 [astro-ph.SR]
- [27] David, T.J., Angus, R., Curtis, J.L., van Saders, J.L., Colman, I.L., Contardo, G., Lu, Y., Zinn, J.C.: Further Evidence of Modified Spin-down in Sun-like Stars: Pileups in the Temperature-Period Distribution. *ApJ* **933**(1), 114 (2022) <https://doi.org/10.3847/1538-4357/ac6dd3> arXiv:2203.08920 [astro-ph.SR]
- [28] Cao, L., Pinsonneault, M.H., van Saders, J.L.: Core-envelope Decoupling Drives Radial Shear Dynamos in Cool Stars. *ApJ* **951**(2), 49 (2023) <https://doi.org/10.3847/2041-8213/acd780> arXiv:2301.07716 [astro-ph.SR]
- [29] Winters, J.G., Henry, T.J., Jao, W.-C., Subasavage, J.P., Chatelain, J.P., Slatten, K., Riedel, A.R., Silverstein, M.L., Payne, M.J.: The Solar Neighborhood. XLV.

- The Stellar Multiplicity Rate of M Dwarfs Within 25 pc. *AJ* **157**(6), 216 (2019) <https://doi.org/10.3847/1538-3881/ab05dc> arXiv:1901.06364 [astro-ph.SR]
- [30] Barnes, S.A.: On the rotational evolution of solar-and late-type stars, its magnetic origins, and the possibility of stellar gyrochronology. *The Astrophysical Journal* **586**(1), 464 (2003)
- [31] Tuomi, M., Jones, H.R.A., Butler, R.P., Arriagada, P., Vogt, S.S., Burt, J., Laughlin, G., Holden, B., Shectman, S.A., Crane, J.D., Thompson, I., Keiser, S., Jenkins, J.S., Berdiñas, Z., Diaz, M., Kiraga, M., Barnes, J.R.: Frequency of planets orbiting M dwarfs in the Solar neighbourhood. arXiv e-prints, 1906-04644 (2019) <https://doi.org/10.48550/arXiv.1906.04644> arXiv:1906.04644 [astro-ph.EP]
- [32] Mohanty, S., Basri, G.: Rotation and Activity in Mid-M to L Field Dwarfs. *ApJ* **583**(1), 451–472 (2003) <https://doi.org/10.1086/345097> arXiv:astro-ph/0201455 [astro-ph]
- [33] Mohanty, S., Basri, G., Shu, F., Allard, F., Chabrier, G.: Activity in Very Cool Stars: Magnetic Dissipation in Late M and L Dwarf Atmospheres. *ApJ* **571**(1), 469–486 (2002) <https://doi.org/10.1086/339911> arXiv:astro-ph/0201518 [astro-ph]
- [34] Kotorashvili, K., Blackman, E.G., Owen, J.E.: Why the observed spin evolution of older-than-solar-like stars might not require a dynamo mode change. *Monthly Notices of the Royal Astronomical Society* **522**(1), 1583–1590 (2023)
- [35] Parker, E.N.: Dynamics of the Interplanetary Gas and Magnetic Fields. *ApJ* **128**, 664 (1958) <https://doi.org/10.1086/146579>
- [36] Weber, E.J., Davis, L. Jr.: The Angular Momentum of the Solar Wind. *ApJ* **148**, 217–227 (1967) <https://doi.org/10.1086/149138>
- [37] Blackman, E.G., Field, G.B.: New Dynamical Mean-Field Dynamo Theory and Closure Approach. *Physical Review Letters* **89**(26), 265007 (2002) <https://doi.org/10.1103/PhysRevLett.89.265007> astro-ph/0207435
- [38] Blackman, E.G., Brandenburg, A.: Doubly Helical Coronal Ejections from Dynamos and Their Role in Sustaining the Solar Cycle. *ApJ* **584**, 99–102 (2003) <https://doi.org/10.1086/368374> astro-ph/0212010
- [39] Blackman, E.G., Thomas, J.H.: Explaining the observed relation between stellar activity and rotation. *MNRAS* **446**, 51–55 (2015) <https://doi.org/10.1093/mnras/slu163> arXiv:1407.8500 [astro-ph.SR]
- [40] Hearn, A.G.: The energy balance and mass loss of stellar coronae. *Astron. & Astrophys.* **40**, 355–364 (1975)

- [41] Kotorashvili, K., Blackman, E.G., Owen, J.E.: Correction to: Why the observed spin evolution of older-than-solar-like stars might not require a dynamo mode change. *MNRAS* **531**(1), 271–271 (2024) <https://doi.org/10.1093/mnras/stae1209>
- [42] Lamers, H.J.G.L.M., Cassinelli, J.P.: *Introduction to Stellar Winds*, (Cambridge Univ. Press, 1999)
- [43] Cranmer, S.R.: New views of the solar wind with the Lambert W function. *American Journal of Physics* **72**(11), 1397–1403 (2004) <https://doi.org/10.1119/1.1775242> [arXiv:astro-ph/0406176](https://arxiv.org/abs/astro-ph/0406176) [astro-ph]
- [44] Goupil, M.-J., Zahn, J.-P.: Tidal dissipation in binary systems. *European Astronomical Society Publications Series* **29**, 67–90 (2008)
- [45] Rozelot, J.-P., Neiner, C.E.: *The Environments of the Sun and the Stars* vol. 857, (Springer Verlag, 2013). <https://doi.org/10.1007/978-3-642-30648-8>
- [46] Tassoul, J.-L.: *Stellar Rotation*, (Cambridge Univ. Press, 2000). <https://doi.org/10.1017/CBO9780511546044>
- [47] Siess, L., Livio, M.: The accretion of brown dwarfs and planets by giant stars - II. Solar-mass stars on the red giant branch. *MNRAS* **308**(4), 1133–1149 (1999) <https://doi.org/10.1046/j.1365-8711.1999.02784.x> [arXiv:astro-ph/9905235](https://arxiv.org/abs/astro-ph/9905235) [astro-ph]
- [48] Nordhaus, J., Spiegel, D.S.: On the orbits of low-mass companions to white dwarfs and the fates of the known exoplanets. *MNRAS* **432**(1), 500–505 (2013) <https://doi.org/10.1093/mnras/stt569> [arXiv:1211.1013](https://arxiv.org/abs/1211.1013) [astro-ph.SR]
- [49] Carlberg, J.K., Smith, V.V., Cunha, K., Majewski, S.R., Rood, R.T.: The Super Lithium-rich Red Giant Rapid Rotator G0928+73.2600: A Case for Planet Accretion? *ApJ* **723**(1), 103–107 (2010) <https://doi.org/10.1088/2041-8205/723/1/L103> [arXiv:1010.2954](https://arxiv.org/abs/1010.2954) [astro-ph.SR]
- [50] Reiners, A., Schüssler, M., Passetger, V.M.: Generalized Investigation of the Rotation-Activity Relation: Favoring Rotation Period instead of Rossby Number. *ApJ* **794**, 144 (2014) <https://doi.org/10.1088/0004-637X/794/2/144> [arXiv:1408.6175](https://arxiv.org/abs/1408.6175) [astro-ph.SR]
- [51] Wright, N.J., Newton, E.R., Williams, P.K.G., Drake, J.J., Yadav, R.K.: The stellar rotation-activity relationship in fully convective M dwarfs. *MNRAS* **479**(2), 2351–2360 (2018) <https://doi.org/10.1093/mnras/sty1670> [arXiv:1807.03304](https://arxiv.org/abs/1807.03304) [astro-ph.SR]
- [52] Nichols-Fleming, F., Blackman, E.G.: Determination of the star-spot covering fraction as a function of stellar age from observational data.

MNRAS **491**(2), 2706–2714 (2020) <https://doi.org/10.1093/mnras/stz3197>
[arXiv:1909.03183](https://arxiv.org/abs/1909.03183) [astro-ph.SR]

- [53] Claret, A.: Theoretical tidal evolution constants for stellar models from the pre-main sequence to the white dwarf stage. Apsidal motion constants, moment of inertia, and gravitational potential energy. *A&A* **674**, 67 (2023) <https://doi.org/10.1051/0004-6361/202346250> [arXiv:2305.01627](https://arxiv.org/abs/2305.01627) [astro-ph.SR]